Complex quasivibrational energy formalism for intensefield multiphoton and abovethreshold dissociation: Complexscaling Fouriergrid Hamiltonian method

Shihl Chu

Citation: The Journal of Chemical Physics **94**, 7901 (1991); doi: 10.1063/1.460125
View online: http://dx.doi.org/10.1063/1.460125
View Table of Contents: http://scitation.aip.org/content/aip/journal/jcp/94/12?ver=pdfcov
Published by the AIP Publishing

Complex quasivibrational energy formalism for intense-field multiphoton and above-threshold dissociation: Complex-scaling Fourier-grid Hamiltonian method

Shih-I Chu
Department of Chemistry, University of Kansas, Lawrence, Kansas 66045

(Received 9 July 1990; accepted 7 March 1991)

We present a new complex-scaling Fourier-grid Hamiltonian (CSFGH) method for accurate and efficient determination of laser-induced (multichannel) molecular resonance states without the use of basis set expansions. The method requires neither the computation of potential matrix elements nor the imposition of boundary conditions, and the eigenvectors provide directly the values of the resonance wave functions at the space grid points. The procedure is particularly valuable for excited-state problems where basis set expansion methods face the challenge. The simplicity and usefulness of the CSFGH method is demonstrated by a case study of the intensity-dependent *complex* quasivibrational energy eigenvalues (E_R, $-\Gamma/2$) and eigenvectors associated with multiphoton and above-threshold dissociation of H_2^+ ions in the presence of intense laser fields ($I = 10^{12}$–10^{14} W/cm^2).

I. INTRODUCTION

It has long been known that multiphoton dissociation (MPD) of polyatomic molecules is an efficient process and can occur in relatively weak infrared laser fields.[1,2] In contrast, MPD of small molecules, particularly diatomic molecules, is a very slow and inefficient process, due to the low density and anharmonicity of vibrational states. Indeed, MPD of diatomic molecules from the *ground* vibrational states of diatomic molecules has never been observed experimentally until 1986. The only exception, as far as diatomic molecules are concerned, is the observation of two-photon dissociation from highly *excited* vibrational states of HD^+.[3] Theoretical studies have shown that MPD from the weaker-bound *high* vibrational levels is far more efficient than from those (tighter-bound) low-lying levels.[4,5]

Due to the recent advent of high power lasers, with intensities ranging from 10^{12} to 10^{15} W/cm^2 (peak electric fields up to 10 V/Å) readily achievable, there is a rapidly growing new interest[6–9] in the study of nonlinear multiphoton dynamics in small molecules, notably molecular hydrogen.[6–9] The latter process involves multiphoton ionization (MPI) of H_2 followed by multiphoton dissociation of H_2^+. A particularly interesting and novel nonlinear optical phenomenon is the observation of the so-called *above-threshold dissociation* (ATD), a process where molecules can absorb more photons than necessary to dissociate the chemical bond. The appearance of equally-spaced multiple peaks in the fragment dissociation spectrum is analogous to the observation of additional peaks in the electron spectra [a phenomenon called *above-threshold ionization* (ATI)] widely studied in the multiphoton ionization of atoms.[10] In addition, chemical bonds can be "softened" in the presence of intense fields, leading to efficient dissociation of nearly all of the vibrational levels.[8] The presence of additional interatomic degrees of freedom in molecules thus enrich the problem of the nonlinear interaction of molecules with intense laser fields.

Considerable theoretical works have been advanced in the description of molecular photoabsorption and laser-induced resonances in the presence of strong laser fields. These can be roughly divided into time-independent basis set expansion or scattering methods[4,9,11,12(a),13] and time-dependent wave packet propagation methods.[12(b)] For the study of MPD of molecules, we have previously developed two theoretical methods.[4,11] The first method, called the *complex quasivibrational energy* (QVE) formalism,[11] is a nonperturbative approach based on the generalization of the Floquet theory[14] to include the complete set of continuum as well as bound vibronic states. This has the effect of giving each of the dressed vibronic levels an intensity-dependent part (width) in addition to the usual field-induced A. C. Stark shifts. Proper examination of the frequency and intensity dependence of these complex QVEs gives rise to rates for MPD processes and is equivalent to infinite-order perturbation theory, self-consistent in that shifts and widths of all levels are simultaneously determined. The second approach[4] is an extension of the inhomogeneous differential equation (IDE) of Dalgarno and Lewis[15] for numerical evaluation of the infinite sum over intermediate states. The IDE method was found to be powerful for weak-field nonresonant MPD calculations.

The purpose of this paper is twofold. Firstly, we introduce a new complex-scaling Fourier-grid Hamiltonian (CSFGH) method for efficient and reliable calculation of the complex quasivibrational energies (resonance energies and widths) in intense laser fields for arbitrary (low-lying or highly excited) vibrational states. In addition to its extreme simplicity in the numerical implementation, namely, *no* potential matrix element computation is required, the method allows *direct* determination of the amplitude of the resonance wave functions at the space grid points. Secondly, we perform a case study of the intensity-dependent complex quasienergy eigenvalues and resonance wave functions associated with the MPD/ATD of H_2^+ ions in intense laser fields, a subject of much current interest both theoretically and experimentally.[6–9]

In the following section (Sec. II), we shall first review

the essence of the complex quasivibrational energy formalism for the problem of MPD/ATD. In Sec. III, we introduce a complex-scaling coupled-channel Fourier-grid Hamiltonian method for the numerical solution of the complex QVEs. The utility and power of this method is illustrated in Sec. IV by a detailed study of the quasivibrational energy resonances associated with MPD/ATD of H_2^+ in high-intensity laser fields.

II. COMPLEX QUASIVIBRATIONAL ENERGY FORMALISM FOR MPD/ATD

The complex quasivibrational energy formalism was introduced previously by the author[11] and co-workers[4] for the study of intense-field molecular photodissociation[11] and two-photon dissociation of diatomic molecules (H_2^+ and HD^+) from excited vibrational levels.[4,5] For the sake of completeness and notation, we briefly outline the formalism below.

Consider the Schrödinger equation for a molecular system in a (single-mode) electromagnetic (EM) field,

$$i\hbar\partial\psi(\mathbf{r},\mathbf{R},t)/\partial t = \hat{H}(\mathbf{r},\mathbf{R},t)\psi(\mathbf{r},\mathbf{R},t), \tag{1}$$

where $\mathbf{r}$ and $\mathbf{R}$ stand for electronic and nuclear coordinates respectively, and the semiclassical time-dependent Hamiltonian $\hat{H}$, in the electric dipole approximation, is given by

$$\hat{H}(\mathbf{r},\mathbf{R},t) = \hat{H}(\mathbf{r},\mathbf{R}) + \boldsymbol{\mu}(\mathbf{r},\mathbf{R})\cdot\boldsymbol{\epsilon}_0\cos(\omega t). \tag{2}$$

Here,

$$\hat{H}(\mathbf{r},\mathbf{R}) = \hat{T}_R + \hat{H}_{\rm el}(\mathbf{r},\mathbf{R}) \tag{3}$$

is the field-free total Hamiltonian (with $\hat{T}_R$ and $\hat{H}_{\rm el}$ being the nuclear kinetic energy operator and the electronic Hamiltonian, respectively), $\mu(\mathbf{r},\mathbf{R})$ is the dipole moment operator, ϵ_0 is the electric field amplitude, and ω is the EM frequency. Consider now the solution of Eq. (1) by expanding $\psi(\mathbf{r},\mathbf{R},t)$ in terms of the field-free basis $\{\xi_\kappa\}$,

$$\psi(\mathbf{r},\mathbf{R},t) = \sum_\kappa a_\kappa(t)\xi_\kappa(\mathbf{r},\mathbf{R}), \tag{4}$$

where $\xi_\kappa(\mathbf{r},\mathbf{R})$ is the solution of the field-free Schrödinger equation

$$\hat{H}(\mathbf{r},\mathbf{R})\xi_\kappa(\mathbf{r},\mathbf{R}) = E_\kappa^{(0)}\xi_\kappa(\mathbf{r},\mathbf{R}). \tag{5}$$

In accordance with the Born–Oppenheimer approximation, one can consider $\mathbf{R}$ as a slowly varying parameter, and the solution of Eq. (5) can be written as

$$\xi_\kappa(\mathbf{r},\mathbf{R}) = \chi_\kappa(\mathbf{R})\psi_\kappa(\mathbf{r},\mathbf{R}), \tag{6}$$

where $\chi_\kappa(\mathbf{R})$ and $\psi_\kappa(\mathbf{r},\mathbf{R})$ are the nuclear and electronic wave functions, respectively. In the *adiabatic* representation, the electronic wave function $\psi_\kappa(\mathbf{r},\mathbf{R})$ is an eigenfunction of $\hat{H}_{\rm el}(\mathbf{r},\mathbf{R})$ with eigenvalue $U_\kappa(\mathbf{R})$, i.e.,

$$\hat{H}_{\rm el}(\mathbf{r},\mathbf{R})\psi_\kappa(\mathbf{r},\mathbf{R}) = U_\kappa(\mathbf{R})\psi_\kappa(\mathbf{r},\mathbf{R}). \tag{7}$$

We shall assume (ψ_κ) forms a complete orthonormal set.

Substituting Eq. (4) into Eq. (1), multiplying both sides by $\xi_j^*(\mathbf{r},\mathbf{R}) \equiv \chi_j^*(\mathbf{R})\psi_j^*(\mathbf{r},\mathbf{R})$ and integrating over $d\mathbf{r}\,d\mathbf{R}$, we find

$$\frac{i\hbar da_j(t)}{dt} = a_j(t)\langle\chi_j(\mathbf{R})|T_R + U_j(\mathbf{R})|\chi_j(\mathbf{R})\rangle + \sum_\kappa a_\kappa(t)\langle\chi_j(\mathbf{R})|\boldsymbol{\mu}_{j\kappa}(\mathbf{R})\cdot\boldsymbol{\epsilon}_0|\chi_\kappa(\mathbf{R})\rangle\cos\omega t, \quad (j,\kappa = 1,2,\ldots). \tag{8}$$

For the case of H_2^+, only two electronic states ($1s\sigma_g$ and $2p\sigma_u$) will be relevant here (Fig. 1), and Eq. (8) reduces to

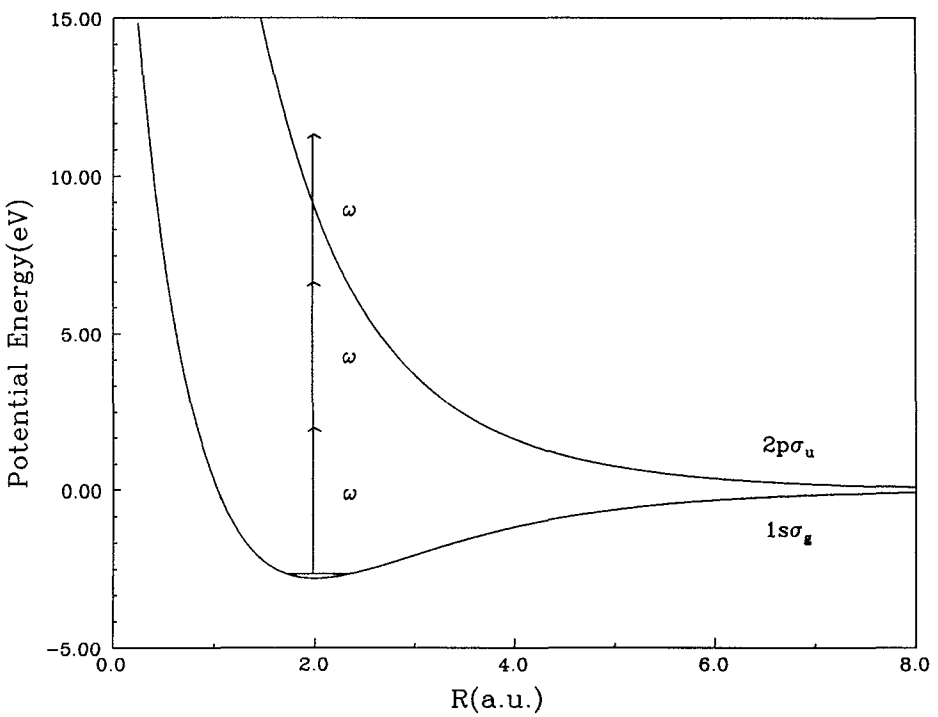

FIG. 1. Potential-energy curves for the ground ($1s\sigma_g$) and first excited ($2p\sigma_u$) states of H_2^+ as a function of internuclear separation R. Also displayed is a schematic diagram showing the absorption of one, two, and three photons of wavelength 2660 Å from the ground vibrational level of the ($1s\sigma_g$) state.

$$i\hbar\frac{d}{dt}\begin{pmatrix}a_1(t)\\a_2(t)\end{pmatrix} = \begin{pmatrix}\langle\chi_1|H_1|\chi_1\rangle & 2\langle\chi_1|V_{12}|\chi_2\rangle\cos\omega t\\ 2\langle\chi_2|V_{21}|\chi_1\rangle\cos\omega t & \langle\chi_2|H_2|\chi_2\rangle\end{pmatrix} \times\begin{pmatrix}a_1(t)\\a_2(t)\end{pmatrix}, \tag{9}$$

where

$$H_\alpha(\mathbf{R}) = T_R + U_\alpha(\mathbf{R}),$$

$$V_{\alpha\beta}(\mathbf{R}) = \frac{1}{2}\boldsymbol{\mu}_{\alpha\beta}(\mathbf{R})\cdot\boldsymbol{\epsilon}_0, \quad (\alpha,\beta = 1,2),$$

and $\boldsymbol{\mu}_{\alpha\beta}(\mathbf{R})$ is the electronic transition dipole moment defined by

$$\boldsymbol{\mu}_{\alpha\beta}(\mathbf{R}) = \int d\mathbf{r}\,\psi^*_\alpha(\mathbf{r},\mathbf{R})\boldsymbol{\mu}(\mathbf{r},\mathbf{R})\psi_\beta(\mathbf{r},\mathbf{R}).$$

[The determination of $U_\alpha(\mathbf{R})$ and $\mu_{\alpha\beta}(\mathbf{R})$ can be performed by standard electronic structure calculations and is not the subject of this paper. The explicit forms of $U_\alpha(\mathbf{R})$ and $\mu_{\alpha\beta}(\mathbf{R})$ for H_2^+ are given in Sec. IV.]

Since the Hamiltonian is periodic in time, eq. (9) can be transformed into an equivalent time-independent infinite-dimensional Floquet Hamiltonian ($\hat{H}_F$) eigenvalue problem:[11,13,14]

$$\hat{H}_F(\mathbf{R})\phi(\mathbf{R}) = \epsilon\phi(\mathbf{R}), \tag{10}$$

where ϵ and $\phi(\mathbf{R})$ are the quasivibrational energy (QVE) eigenvalues and eigenvectors, respectively. In terms of the Floquet-state basis

$$|\alpha,n\rangle = |\alpha\rangle\times|n\rangle,$$

where $|\alpha\rangle$ denotes the electronic states, and n is the photon Fourier index (ranging from $-\infty$ to $+\infty$), the Floquet Hamiltonian $\hat{H}_F$ has the following form:[11]

$$(\hat{H}_F)_{\alpha n,\beta m} = [T_R + U_\alpha(\mathbf{R}) + n\hbar\omega]\delta_{\alpha\beta}\delta_{nm} + [\tfrac{1}{2}\boldsymbol{\mu}_{\alpha\beta}(\mathbf{R})\cdot\boldsymbol{\epsilon}_0]\delta_{n,m=n\pm1}\cdot(1-\delta_{\alpha\beta}). \tag{11}$$

In the case of two electronic states, for example, the Floquet Hamiltonian $\hat{H}_F$ has the structure shown in Fig. 2. We see $\hat{H}_F$ has a periodic structure with only the number of ω's in the diagonal elements varying from block to block. The structure endows the eigenvalues and eigenvectors of $\hat{H}_F$ with periodic properties. [In Eq. (11) and Fig. 2, we have expressed the electric dipole interaction in the length form. An alternative expression in terms of the velocity form will be discussed in Sec. IV. Both forms lead to the same results, if performed exactly.]

The Floquet matrix so constructed is a real, symmetric matrix and contains no discrete spectrum in the real energy axis. Writing the time evolution operator in the form,

$$\exp(-i\hat{H}_F t/\hbar) = \frac{1}{2\pi i}\int_c dz\exp(-izt/\hbar)\cdot(z-\hat{H}_F)^{-1}, \tag{12}$$

gives the usual result that the time dependence is dominated by poles of $(z-\hat{H}_F)^{-1}$ near the real axis but on higher Riemann sheets, and the complex energies of the poles are related to the positions and widths of the shifted and broadened quasienergy states. These complex pole positions may be found directly from the analytically continued Floquet Hamiltonian $\hat{H}_F(\theta)$ obtained by applying the complex scaling transformation[16,17] to the nuclear coordinate, $\mathbf{R}$, $\mathbf{R}\rightarrow\mathbf{R}\exp(i\theta)$. This dilatation transformation effects an analytic continuation of $(z-\hat{H}_F)^{-1}$ into the lower half-plane on appropriate higher Riemann sheets, allowing the complex quasienergy states (now become square integrable) to be determined by solution of a nonHermitean eigenvalue problem. In practice, the diagonal electronic blocks $H_\alpha[\mathbf{R}\exp(i\theta)]$ may be expanded and discretized by the use of appropriate L^2 (square integrable) radial (vibrational) basis as has been performed in previous studies.[4,11] The desired complex quasivibrational energies (QVEs) are then identified by the stationary points[11] of the θ trajectories of the eigenvalues of $\hat{H}_F(\theta)$. Once the QVEs and their corresponding eigenstates are found, the intensity- and time-dependent (multiphoton) photodissociation rates can also be determined. We refer the readers to Ref. 11 for detailed discussion on these points. Similar complex quasienergy formalism has been developed for the study of multiphoton ionization[18] and above-threshold ionization[19] of atoms in intense laser fields.

In the following section, we shall introduce an alternative procedure for the solution of the complex QVEs without the need of using basis set expansion and the computation of potential matrix elements.

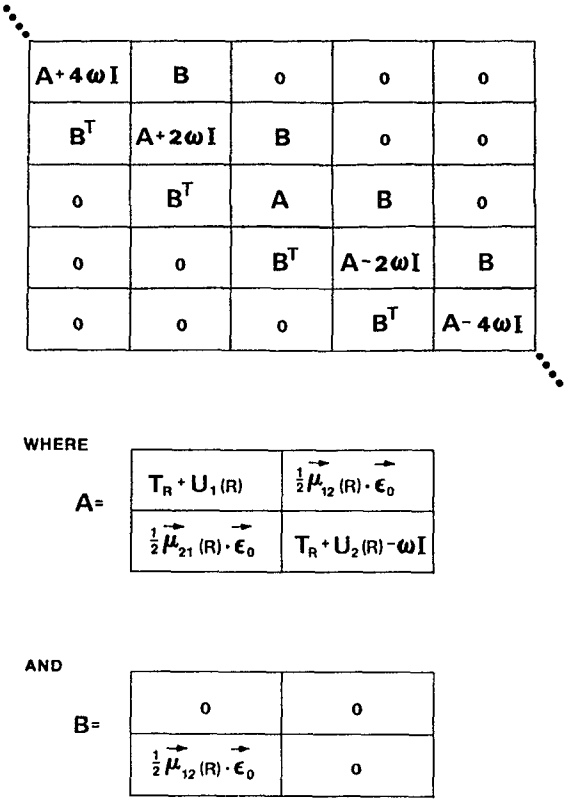

FIG. 2. Structure of the Floquet Hamiltonian $\hat{H}_F$ for MPD/ATD.

III. COMPLEX-SCALING COUPLED-CHANNEL FOURIER-GRID HAMILTONIAN METHOD

In a recent communication,[20] we have discussed a new complex scaling procedure for the study of (one-channel) resonance eigenstates without the use of basis set expansions. The procedure does not require the computation of potential matrix elements (which is usually the most time consuming part) and in addition the eigenvectors provide directly the values of resonance wave functions at the space grid points. The method makes use of the recent advancement of the calculation of bound state eigenvalues and eigenfunctions using the Fourier transform method.[21] It has been pointed out that the complex-scaling Fourier grid Hamiltonian (CSFGH) method is particularly valuable for highly excited state problems where the basis set expansion methods face the difficulties.[20] The purpose of this section is to show how the CSFGH procedure may be extended to multichannel resonance state problems.

It is known that the kinetic energy operator ($\hat{T}_R$ in this case) is best represented in the momentum representation.[21] Since

$$\langle \mathbf{k}'|\hat{T}_R|\mathbf{k}\rangle = (\hbar^2 k^2/2\mu)\delta(\mathbf{k}-\mathbf{k}'), \tag{13}$$

$\hat{T}_R$ is diagonal in the $|\mathbf{k}\rangle$ representation. Here $|\mathbf{k}\rangle$ are the eigenfunctions of $\hat{P}$, namely,

$$\hat{P}|\mathbf{k}\rangle = \hbar\mathbf{k}|\mathbf{k}\rangle,$$

and satisfy the orthonormal and completeness relationships, respectively,

$$\langle \mathbf{k}|\mathbf{k}'\rangle = \delta(\mathbf{k}-\mathbf{k}') \tag{14}$$

and

$$\hat{I}_{\mathbf{k}} = \int_{-\infty}^{\infty} |\mathbf{k}\rangle\langle\mathbf{k}|d\mathbf{k}. \tag{15}$$

On the other hand, the potential energy term ($\hat{U}_\alpha(\mathbf{R})$, $\alpha = 1,2$) is diagonal in the coordinate representation,

$$\langle \mathbf{R}'|\hat{U}_\alpha(\mathbf{R})|\mathbf{R}\rangle = U_\alpha(\mathbf{R})\delta(\mathbf{R}-\mathbf{R}'). \tag{16}$$

Here $|\mathbf{R}\rangle$ are the eigenfunctions of the coordinate operator,

$$\hat{\mathbf{R}}|\mathbf{R}\rangle = \mathbf{R}|\mathbf{R}\rangle, \tag{17}$$

and satisfy the relationships,

$$\langle \mathbf{R}|\mathbf{R}'\rangle = \delta(\mathbf{R}-\mathbf{R}') \tag{18}$$

and

$$\hat{I}_{\mathbf{R}} = \int_{-\infty}^{\infty} |\mathbf{R}\rangle\langle\mathbf{R}|d\mathbf{R}. \tag{19}$$

In the coordinate or Schrödinger representation, the complex-scaling Hamiltonian operators in the diagonal Floquet blocks (c.f. Fig. 2) become

$$\begin{aligned}\langle \mathbf{R}|\hat{H}_\alpha(\mathbf{R}e^{i\theta})|\mathbf{R}'\rangle &\equiv \langle \mathbf{R}|e^{-2i\theta}\hat{T}_R + \hat{U}_\alpha(\mathbf{R}e^{i\theta})|\mathbf{R}'\rangle \\ &= e^{-2i\theta}\langle \mathbf{R}|\hat{T}_R|\mathbf{R}'\rangle + U_\alpha(\mathbf{R}e^{i\theta})\delta(\mathbf{R}-\mathbf{R}'), \\ &\quad (\alpha = 1,2).\end{aligned} \tag{20}$$

Using the identity operator in Eq. (15), the kinetic energy operator term in Eq. (20) can be rewritten as

$$\langle \mathbf{R}|\hat{T}_R|\mathbf{R}'\rangle = (1/2\pi)\int_{-\infty}^{\infty} e^{i\mathbf{k}\cdot(\mathbf{R}-\mathbf{R}')}T_k\,d\mathbf{k}, \tag{21}$$

where $T_k = \hbar^2 k^2/2\mu$, and μ is the reduced mass of the molecular system.

Without loss of generality, we shall assume $\boldsymbol{\mu}_{12}(\mathbf{R})//\boldsymbol{\epsilon}_0$ in the following. Thus $R(\equiv|\mathbf{R}|)$, the internuclear separation, will be treated as a scalar parameter. To discretize the continuous range of coordinate value R, we adopt the Fourier grid method.[21] Here a uniform discrete spatial grid

$$R_j = j\Delta R \quad (j = 1,2,\ldots,N) \tag{22}$$

will be used where N is an *odd* integer number. The orthogonality condition, Eq. (18), and the identity operator, Eq. (19), may now be written as

$$\Delta R\,\langle R_j|R_{j'}\rangle = \delta_{jj'} \tag{23}$$

and

$$\hat{I}_R = \sum_{j=1}^{N} |R_j\rangle\Delta R\,\langle R_j|. \tag{24}$$

The grid size and spacing in the coordinate space determines the reciprocal grid size in the momentum space. Thus $\Delta k = 2\pi/N\Delta R$. The central point in the momentum space grid is chosen to be $k = 0$, and the grid's points are evenly distributed about zero.

The discretized version of the complex-scaling Hamiltonian operators in the diagonal Floquet blocks now has the following form (after some simplification)

$$\begin{aligned}\langle R_j|\hat{H}_\alpha(Re^{i\theta})|R_{j'}\rangle &= (2e^{-2i\theta}/N)\sum_{l=1}^{L}\cos[2\pi l(j-j')/N]\,T_l \\ &\quad + U_\alpha(R_j e^{i\theta})\delta_{jj'},\end{aligned} \tag{25}$$

where $L = (N-1)/2$, $T_l = (2/\mu)(\hbar\pi l/N\Delta R)^2$, and $\alpha = 1,2$. The electric-dipole coupling operator in the off-diagonal Floquet blocks (Fig. 2) can be similarly readily computed, as it is also diagonal in the coordinate representation. The discretized version of the complex-scaling Floquet Hamiltonian, Eq. (11), thus now becomes

$$\begin{aligned}\langle R_j|[\hat{H}_F(Re^{i\theta})]_{\alpha n,\beta m}|R_{j'}\rangle &= \left\{(2e^{-2i\theta}/N)\sum_{l=1}^{L}\cos[2\pi l(j-j')/N]\,T_l \right. \\ &\quad \left. + [U_\alpha(R_j e^{i\theta}) + n\hbar\omega]\delta_{jj'}\right\}\delta_{\alpha\beta}\delta_{nm} \\ &\quad + \tfrac{1}{2}\boldsymbol{\mu}_{\alpha\beta}(R_j e^{i\theta})\cdot\boldsymbol{\epsilon}_0\delta_{jj'}\delta_{n,m=n\pm1}\cdot(1-\delta_{\alpha\beta}).\end{aligned} \tag{26}$$

This completes the construction of the non-Hermitian Floquet Hamiltonian in the coordinate representation. The complex quasienergy eigenvalues and eigenvectors can now be determined by the solution of the complex secular equations:

$$\sum_{j'}\{[\hat{H}_F(Re^{i\theta})]_{jj'} - W_\nu\delta_{jj'}\}\psi_{j'}^{\nu}(\theta) = 0, \tag{27}$$

where the eigenvectors ψ_j^ν give *directly* the amplitude of the complex quasienergy resonance wave functions ψ^ν evaluated at the grid points R_j,

$$\psi_j^\nu(\theta) = \langle R_j|\psi^\nu(\theta)\rangle = \psi^\nu(R_j e^{i\theta}). \tag{28}$$

TABLE I. Molecular parameters for $U_i(R)$ and $\mu_{12}(R)$.

Potential[a]	D_0 (eV)	$\alpha(a_0^{-1})$	$R_e(a_0)$	t
$U_1(R)$	2.7925	0.72	2.0	1.0
$U_2(R)$	2.7925	0.72	2.0	−1.11
Trans. dipole moment[b]		$\mu(R_e)$	$\mu'(R_e)$	y
$\mu_{12}(R)$		$1.07ea_0$	$0.396e$	−0.055

[a] $U_i(R) = D_0\{\exp[-2\alpha(R-R_e)] - 2t_i \exp[-\alpha(R-R_e)]\}$, $(i=1$ for $1s\sigma_g$ and $i=2$ for $2p\sigma_u)$.
[b] $\mu_{12}(R) = \mu(R_e) + [\mu'(R_e)/\alpha y]\cdot\{1-\exp[-\alpha y(R-R_e)]\}$.

IV. INTENSITY-DEPENDENT COMPLEX QUASIVIBRATIONAL ENERGIES: MULTIPHOTON/ABOVE-THRESHOLD DISSOCIATION OF H_2^+

In this section, we present an application of the complex-scaling coupled-channel Fourier-grid Hamiltonian method to the study of complex quasivibrational energies of H_2^+ undergoing MPD/ATD in intense laser fields. For weak-field single-photon two-electronic-state problem, only the minimal (2×2 block) matrix A shown in Fig. 2 needs to be considered. For stronger fields, a few more Floquet blocks are needed to achieve convergence.[11] As in our previous studies of H_2^+, we shall use the Morse potentials[4,11]

$$U_i(R) = D_0\{\exp[-2\alpha(R-R_e)] - 2t_i\exp[-\alpha(R-R_e)]\}, \quad (i=1,2) \tag{29}$$

for describing both the ground ($1s\sigma_g$) and the excited repulsive ($2p\sigma_u$) electronic states. For the transition dipole moment we adopt[11,22]

$$\mu_{12}(R) = \mu(R_e) + \frac{\mu'(R_e)}{\alpha y}\{1-\exp[-\alpha y(R-R_e)]\}, \tag{30}$$

where $\mu'(R_e)$ is the dipole derivative and y is the electronic anharmonicity. The molecular parameters used for $U_i(R)$ and $\mu_{12}(R)$ are listed in Table I, which were first suggested by Bunkin and Tugov[22] and used recently also by others.[9(a)] Bunkin and Tugov found that the analytical $U_i(R)$ and $\mu_{12}(R)$ given in Eqs. (29) and (30) for short and intermediate range of R are in good agreement with their exact numerical values.[23] Asymptotically ($R\to\infty$), the exact transition dipole moment should become $R/2$.

The laser–molecular interaction described so far is expressed in terms of the length form. An alternative expression of the dipolar interaction can be derived in terms of the velocity form

$$V^v_{\alpha\beta}(R) = -(e/mc)\mathbf{A}\cdot\langle\psi_\alpha(\mathbf{r},\mathbf{R})|\mathbf{P}|\psi_\beta(\mathbf{r},\mathbf{R})\rangle, \tag{31}$$

where $\mathbf{A}$ is the vector potential ($A = c/\omega\epsilon_0$) and $\mathbf{P}$ is the electronic momentum operator. It can be shown readily that the dipolar interaction in the velocity form is related to that in the length form via the relation

$$V^v_{\alpha\beta}(R) = i[(U_\alpha(R) - U_\beta(R))/\hbar\omega]V^L_{\alpha\beta}(R), \tag{32}$$

where $V^L_{\alpha\beta}(R) = -\boldsymbol{\mu}_{\alpha\beta}(R)\cdot\boldsymbol{\epsilon}_0$ is the electric-dipole coupling in the length form. Although the length and the velocity gauges lead to the same results in an exact calculation, it is usually more convenient to use the length form in weak to medium field calculations and more advantageous to use the velocity form for very strong field calculations. This is particularly true for H_2^+ molecule, since $\mu_{12}(R)$ here diverges asymptotically. The use of the velocity gauge leads to, however, vanishing dipolar interaction at large separation R

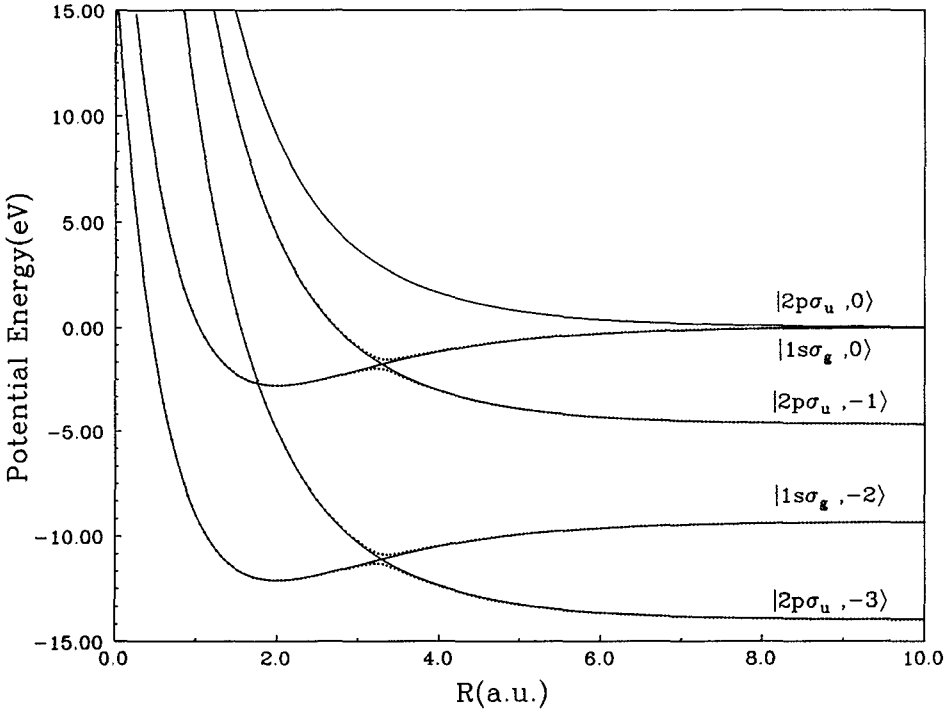

FIG. 3. Electronic-field potential-energy curves of the two electronic states of H_2^+ dressed by $n=0,-1,-2,-3$ photons of wavelength 2660 Å. Solid lines: diabatic curves. Dotted lines: adiabatic curves.

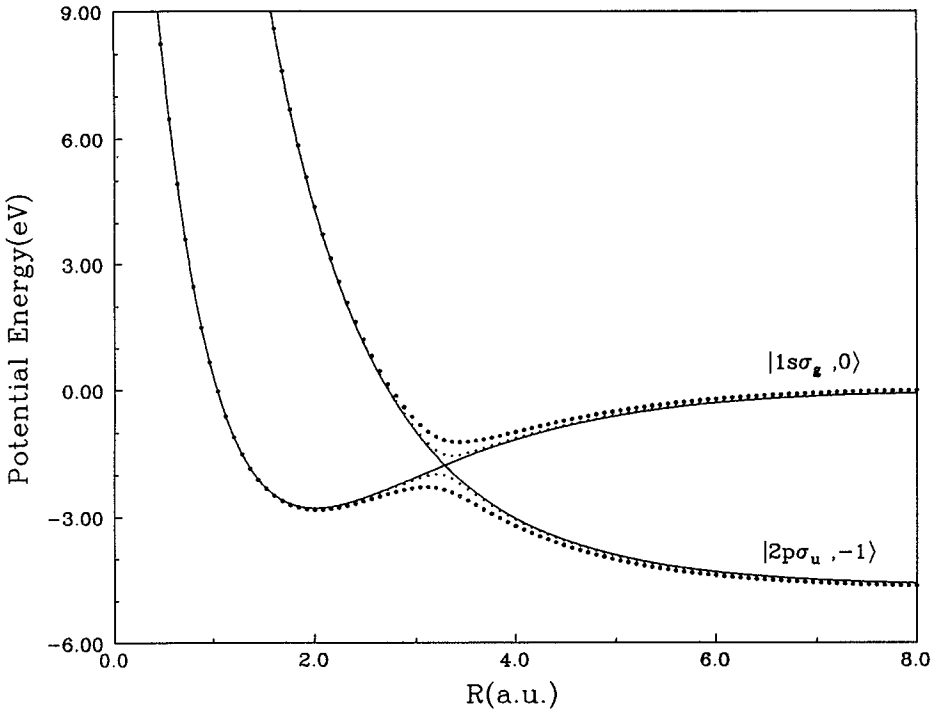

FIG. 4. Intensity-dependent avoided crossing pattern nearby one-photon dominant transition region. ... curve: $F_{rms} = 0.01$ a.u., ooo curve: $F_{rms} = 0.02$ a.u.

(since $U_\alpha(R) - U_\beta(R) \to 0$ as $R \to \infty$), allowing the reduction of the number of coupled channels in strong field calculations. The significance of using the velocity form in MPD/ATD studies has therefore recently gained attention.[9(b),24] In the following discussion, we shall present the results based mainly on the velocity gauge.

The MPD dynamics can be understood in terms of the Floquet electronic-field potential curve crossings. Shown in Fig. 3 are some of the diabatic potential curves (solid lines). Each curve corresponds to $U_i(R) + n\hbar\omega$, where $U_i = 1s\sigma_g$ or $2p\sigma_u$ and $n = 0, -1, -2, -3$ are the Fourier photon indices. When the fields are turned on, these curves become avoided-crossing curves[11] (dotted lines in Fig. 3). Formally, the photodissociation or multiphoton dissociation between a bound and a repulsive electronic states is a half-collision process and can be regarded as a (diabatic) curve-crossing or an (adiabatic) avoided-crossing predissociation problem.[11,25] As pointed out previously,[11,25] the electronic-field surfaces "repel" each other in the avoided crossing regions as the field intensity increases (an example is given in Fig. 4). Fig. 4 serves to illustrate a couple of salient points of MPD processes. Firstly, the initially bound vibrational levels of H_2^+ ($1s\sigma_g$) levels can now tunnel through the potential barrier (the lower branch of adiabatic curves) and become dissociated. Thus all the vibrational levels are now metastable quasivibrational energy states with complex eigenvalues $W = (E_R - \Gamma/2)$, the imaginary widths (Γ) being related to the total MPD rates. Secondly, as the field intensity increases, the "adiabatic" potential barrier gets lower, and fewer (quasibound) vibrational levels can be supported by the $1s\sigma_g$ (distorted) potential well. This phenomenon is termed molecular bond "softening."[8]

Using the complex-scaling Fourier-grid Hamiltonian method described in Sec. III and the velocity-form dipolar coupling, we have computed the complex quasivibrational energies of H_2^+ for $\lambda = 2660$ Å and a range of field intensities. We found 51 space grid points (evenly distributed from $R_{min} = 0.5$ a.u. to $R_{max} = 10$ a.u.) are sufficient to achieve accuracy (for both E_R and $\Gamma/2$) to at least four significant digits even for highly excited states (up to $v = 16$). Higher accuracy can be achieved by increasing the number of mesh points and by adjusting R_{max}. Some of the results are presented below.

Figure 5 shows the photodissociation (half-) widths

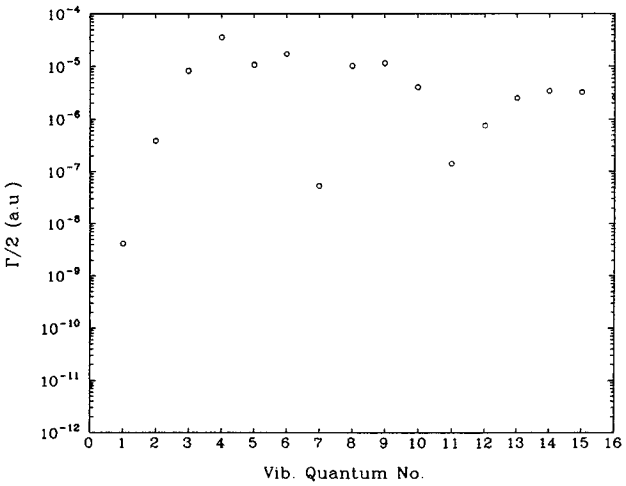

FIG. 5. The photodissociation (half-) widths $\Gamma/2$ ($\equiv -\mathrm{Im}(W)$) of H_2^+ ($1s\sigma_g$) as a function of the initial vibrational quantum number v. The field parameters are $\lambda = 2660$ Å, and $F_{rms} = 0.001$ a.u. At this field strength, the photodissociation is dominantly a one-photon process.

($\Gamma/2 = -Im(W)$) of H_2^+ ($1s\sigma_g$) as a function of the initial vibrational quantum v. The rms field strength (F_{rms}) used is 10^{-3} a.u. (equivalent to 7×10^{10} W/cm^2). At this intensity, the photodissociation is dominated by the one-photon absorption process. The dissociation rate shows a rapid increase by seven orders of magnitude from $v=0$ to $v=4$, followed by some oscillatory behavior. Figure 6 shows the intensity-dependent MPD (half-) widths ($\Gamma/2$) as a function of the laser intensity I for the ground vibrational level ($v=0$) of the H_2^+ ($1s\sigma_g$) electronic state. It is seen that the photodissociation rate increases rapidly with field intensity. The onset of the above-threshold dissociation (ATD) process can be seen more clearly by plotting Γ/F_{rms}^2 (proportional to Γ/I) vs the laser intensity I. This is shown in Fig. 7. At weaker fields, Γ/F_{rms}^2 is seen to be independent of the field intensity I, and the photodissociation is dominantly a one-photon process. Above some critical field intensity ($\approx10^{12}$ W/cm^2), ATD sets in, and the process becomes highly nonlinear. Similar behavior has been observed in other recent nonperturbative studies of this related problem, using the scattering formalism.[9]

It is instructive to study the resonance wave function behavior in the presence of strong fields. As pointed out previously, the eigenvectors (in the Fourier-grid Hamiltonian method)[20,21] provide directly the amplitude of the wave functions at the space grid points. Shown in Fig. 8 are the square of the modulus of the (time-independent) quasivibrational energy eigenstates corresponding to $v=0,1,2,5,10$, and 15 of the H_2^+ ($1s\sigma_g$) electronic state. The field strength used is $F_{rms}=0.001$ a.u., and $\lambda=266$ nm. These wave functions are obtained from diagonalization of the Hermitian Floquet Hamiltonian $\hat{H}_F$ (with velocity-form dipolar coupling) (*without* the use of the complex-scaling transformation) by means of the coupled-channel Fourier-grid Hamiltonian method. As the field intensity ($\approx7\times10^{10}$ W/cm^2) is rather weak, these field-perturbed quasivibrational energy eigenfunctions still mimic rather well the nodal structure of the unperturbed vibrational wave functions of

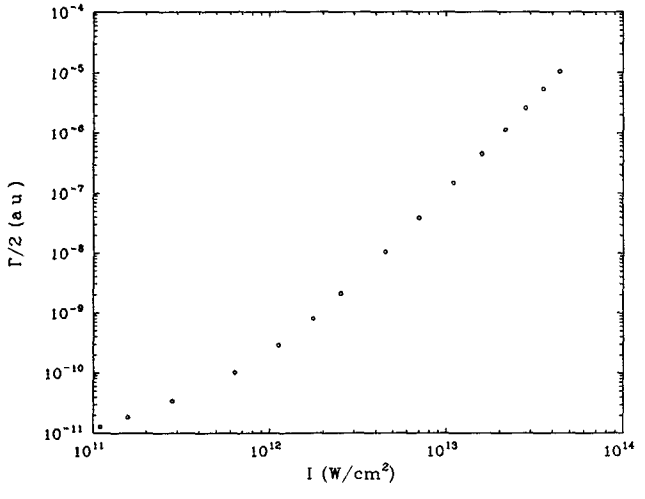

FIG. 6. Intensity-dependent MPD (half-) widths $\Gamma/2$ for the ground vibrational level ($v=0$) of the H_2^+ ($1s\sigma_g$) state at $\lambda=2660$ Å.

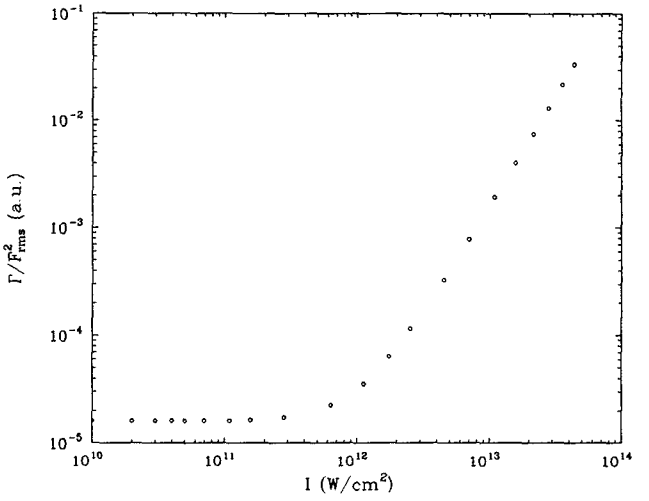

FIG. 7. Reduced widths (Γ/F_{rms}^2) vs intensity I, for the ground vibrational level ($v=0$) of the H_2^+ ($1s\sigma_g$) state at $\lambda=2660$ Å. At weaker fields, the photodissociation is a dominant one-photon process. Above some critical field intensity ($\approx10^{12}$ W/cm^2), MPD/ATD become significant and dominant in the photodissociation process.

H_2^+ ($1s\sigma_g$) state. It is interesting to note that higher members (v) of the quasivibrational energy wave functions carry visibly some continuum (oscillatory) tails. These are bound states set in the continuum.

Figure 9 depicts the corresponding (unnormalized) resonance (i.e., *complex* quasivibrational energy) wave functions obtained by the complex-scaling Fourier-grid Hamiltonian method, under the same field parameter conditions. As can be seen, these resonance wave functions are localized and broadened wave packets, with the vibrational (nodal) oscillatory structure superimposed on the envelope of the wave packets. It is also interesting to examine the effect of intensity on the behavior of resonance wave functions. In Fig. 10, we show the quasivibrational energy wave functions (*without* the use of complex scaling) for $v=0,2$, and 5 of H_2^+ ($1s\sigma_g$) state at 266 nm with the field intensity now increasing to 7×10^{12} W/cm^2. Because of the stronger mixing of the $1s\sigma_g$ and $2p\sigma_u$ states, we see even low-lying excited members (v) of the quasivibrational energy wave functions now carry quite pronounced continuum (oscillatory) tails. The corresponding (unnormalized) resonance (complex quasivibrational energy) wave functions are depicted in Fig. 11 for comparison. Again we see localized (without the continuum tails) and broadened wave packets—a consequence of the complex-scaling transformation.

In summary, we have presented in this paper a new complex-scaling coupled-channel method for efficient and reliable treatment of laser-induced resonance states. The procedure does not require the computation of potential matrix elements and the eigenvectors provide directly the values of the resonance wave functions at the space grid points. The method has the additional advantage (over the basis set expansion method) in that highly excited resonance states can be treated with high accuracy without too much increase in the number of mesh points.

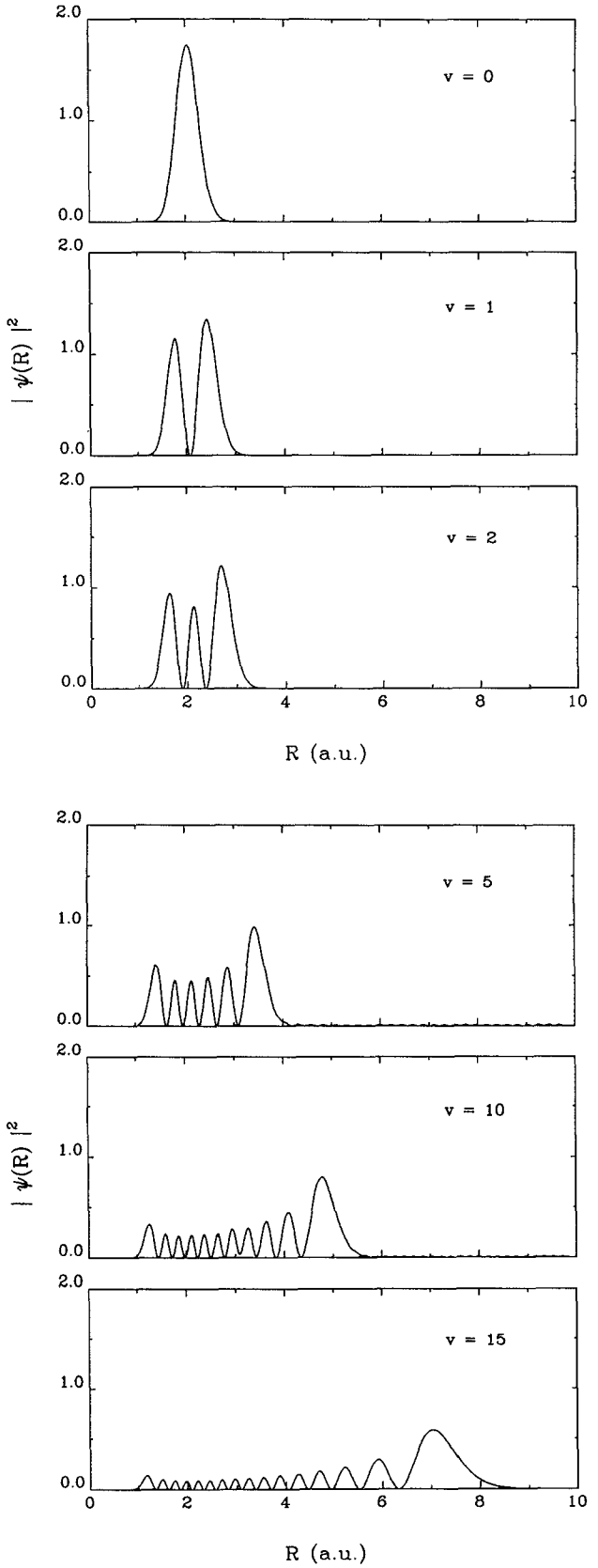

FIG. 8. $|\psi(R)|^2$ vs R for quasivibrational energy wave functions $\psi(R)$ correlated with $v=0,1,2,5,10$, and 15 vibrational levels of H_2^+ $(1s\sigma_g)$ state. $\psi(R)$'s are eigenfunctions of the Hermitian Floquet Hamiltonian $\hat{H}_F$ (in velocity gauge) discretized in the coordinate representation. The field parameters are $I=7\times10^{10}$ W/cm^2 and $\lambda=2660$ Å.

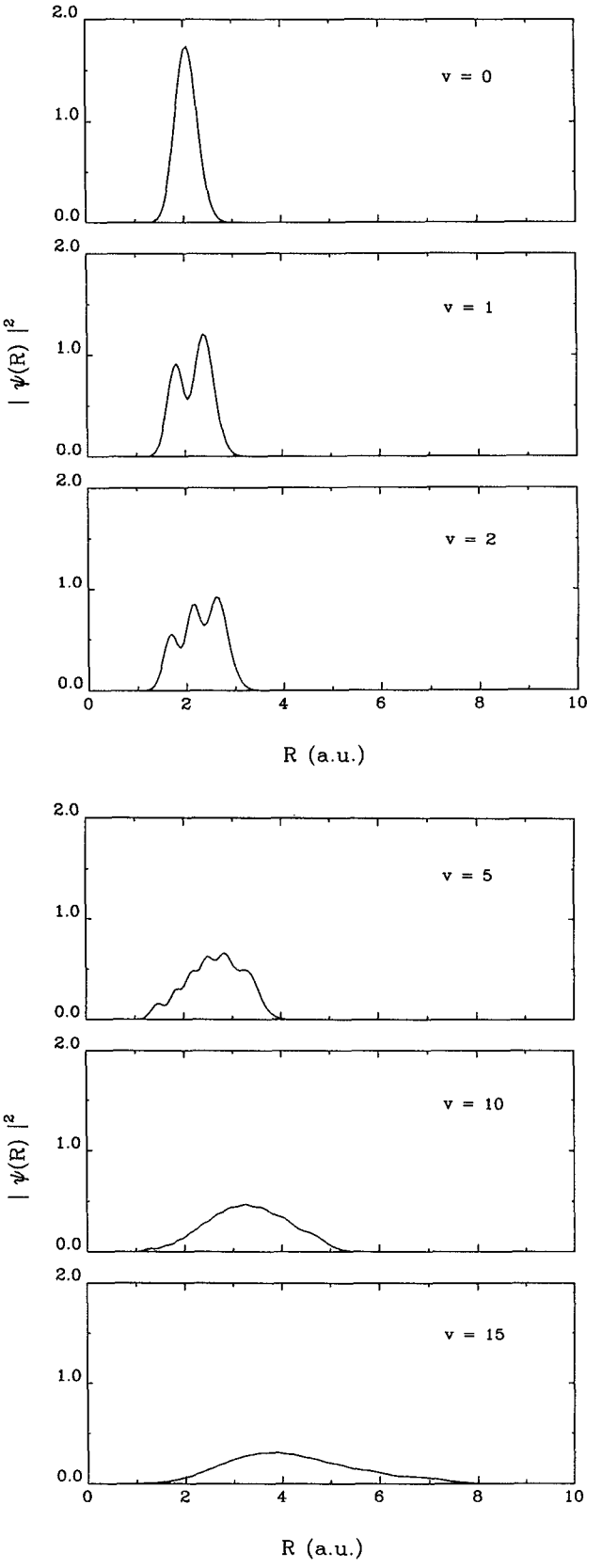

FIG. 9. $|\psi(R)|^2$ vs R for *complex* quasivibrational energy wave functions $\psi(R)$ correlated with $v=0,1,2,5,10$, and 15 vibrational levels of H_2^+ $(1s\sigma_g)$ state. $\psi(R)$'s are the eigenfunctions of the complex-scaling Floquet Hamiltonian $\hat{H}_F(\theta)$ (in velocity gauge). Field parameters are the same as Fig. 8. The rotation angle θ used is 0.08 rad. These resonance states are seen to be localized and broadened wave packets.

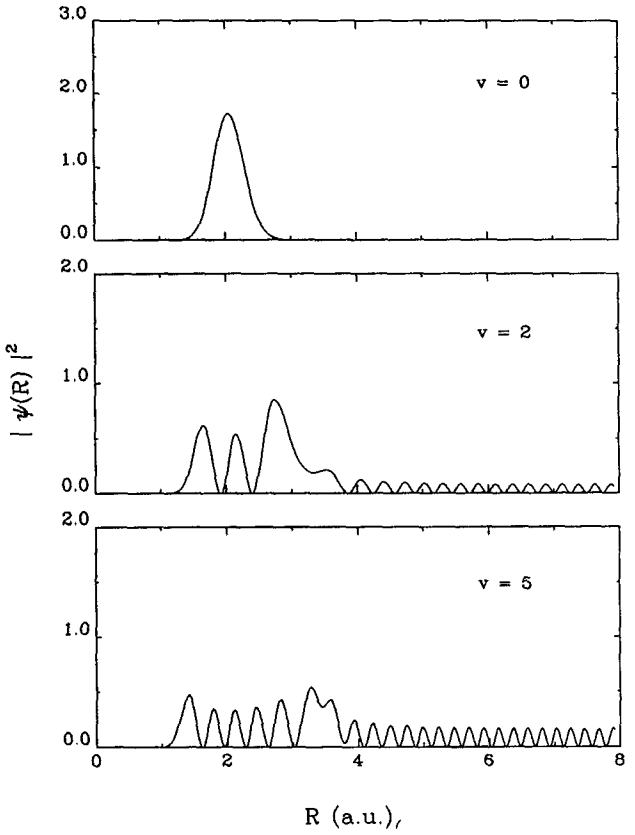

FIG. 10. Same as Fig. 8 except that the field intensity is now increased to $I = 7\times 10^{12}$ W/cm^2 and only quasivibrational energy states with $v = 0$, 2, and 5 are shown. Notice the pronounced continuum tails attached to the bound state wave functions.

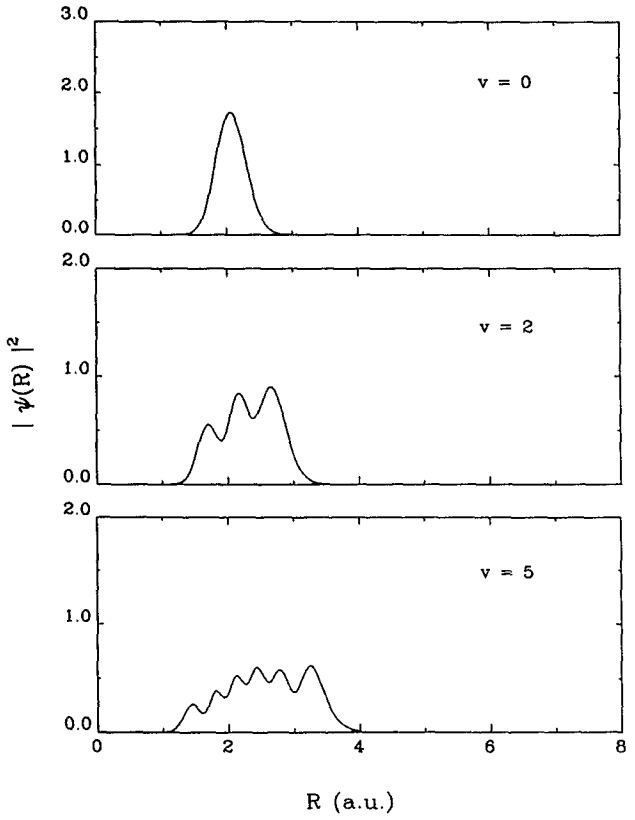

FIG. 11. Same as Fig. 10 except that *complex* quasivibrational-energy resonance states are shown.

We have applied the new procedure to the study of intensity-dependent complex quasivibrational energy eigenvalues and eigenvectors associated with MPD/ATD of H_2^+ in the presence of intense laser fields (10^{12} to 10^{14} W/cm^2). Detailed investigation of the molecular multiphoton dynamics and novel nonlinear optical phenomena (ATD, molecular-bond softening, and harmonic generation, etc.) in very intense laser fields is in progress, and will be discussed elsewhere.

ACKNOWLEDGMENT

This work was partially supported by the Department of Energy (Division of Chemical Sciences).

[1] N. Bloembergen and E. Yablonovitch, Phys. Today **31**, 23 (1978); P. A. Schulz, Aa. S. Sudbo, D. J. Krajnovich, H. S. Kwok, Y. R. Shen, and Y. T. Lee, Annu. Rev. Phys. Chem. **30**, 311 (1979).
[2] See, for example, V. S. Letokhov, *Nonlinear Laser Chemistry* (Springer, New York, 1983); *Photoselective Chemistry*, Advan. Chem. Phys. Vol. **47**, edited by J. Jortner, R. D. Levine, and S. A. Rice (Wiley, New York, 1981); *Advances in Multiphoton Processes and Spectroscopy*, edited by S. H. Lin (World Scientific, Singapore, 1984, 1986, 1988).
[3] A Carrington and J. Buttenshaw, Mol. Phys. **44**, 267 (1981).
[4] S. I. Chu, C. Laughlin, and K. K. Datta, Chem. Phys. Lett. **98**, 476 (1983).
[5] C. Laughlin, K. K. Datta, and S. I. Chu, J. Chem. Phys. **85**, 1403 (1986).
[6] C. Cornaggia, D. Normand, J. Morellec, G. Mainfray, and C. Manus, Phys. Rev. A **34**, 207 (1986); J. W. J. Verschuur, L. D. Noordam, and H. B. van Linden van den Heuvell, Phys. Rev. A **40**, 4383 (1989).
[7] T. S. Luk and C. K. Rhodes, Phys. Rev. A **38**, 6180 (1988).
[8] P. H. Bucksbaum, A. Zavriyev, H. G. Muller, and D. W. Schumacher, Phys. Rev. Lett. **64**, 1883 (1990).
[9] (a) X. He, O. Atabek, and A. Giusti-Sugor, Phys. Rev. A **38**, 5586 (1988); A **42**, 1585 (1990); (b) A. Giusti-Sugor, X. He, O. Atabek, and F. H. Mies, Phys. Rev. Lett. **64**, 515 (1990).
[10] See, for example, P. Agostini, F. Fabre, G. Mainfray, G. Petite, and N. Rahman, Phys. Rev. Lett. **42**, 1127 (1979); P. Kruit, J. Kimman, and M. Van der Wiel, J. Phys. B **14**, L597 (1981); R. R. Freeman, T. J. McIlrath, P. H. Bucksbaum and M. Bashkansky, Phys. Rev. Lett. **57**, 3156 (1986).
[11] S. I. Chu, J. Chem. Phys. **75**, 2215 (1981).
[12] (a) For other time-independent methods for strong field problems, see, for example, T. F. George, J. Phys. Chem. **86**, 10 (1982); A. D. Bandrauk, and G. Turcotte, J. Phys. Chem. **87**, 5098 (1983); K. B. Whaley and J. C. Light, J. Chem. Phys. **77**, 1818 (1982); C. Leforestier and R. E. Wyatt, Phys. Rev. A **25**, 1250 (1982). (b) Time-dependent methods for strong field problems can be found, for example, in R. Heather and H. Metiu, J. Chem. Phys. **88**, 5496 (1988); S. I. Chu and T. F. Jiang, Computer Phys. Comm. **63**, 482 (1991).
[13] S. I. Chu, Adv. At. Mol. Phys. **21**, 197 (1985); Adv. Chem. Phys. **73**, 739 (1989).
[14] J. H. Shirley, Phys. Rev. B **138**, 979 (1965).
[15] A. Dalgarno and J. T. Lewis, Proc. Roy. Soc. A **233**, 70 (1955).
[16] E. Balslev and J. M. Combes, Commun. Math. Phys. **22**, 280 (1971); B. Simon, Ann. Math. **97**, 247 (1973).
[17] B. R. Junker, Adv. At. Mol. Phys. **18**, 208 (1982); W. P. Reinhardt, Annu. Rev. Phys. Chem. **33**, 223 (1982).
[18] S. I. Chu and W. P. Reinhardt, Phys. Rev. Lett. **39**, 1195 (1977); S. I. Chu, Chem. Phys. Lett. **54**, 367 (1978).
[19] S. I. Chu and J. Cooper, Phys. Rev. A **32**, 2769 (1985); S. I. Chu, K. Wang, and E. Layton, J. Opt. Soc. Am. B **7**, 425 (1990).
[20] S. I. Chu, Chem. Phys. Lett. **167**, 155 (1990).
[21] C. C. Marston and G. G. Balint-Kurti, J. Chem. Phys. **91**, 3571 (1989).
[22] F. V. Bunkin and I. I. Tugov, Phys. Rev. A **8**, 601 (1973).
[23] D. R. Bates, J. Chem. Phys. **19**, 1122 (1951); D. R. Bates, K. Ledsham, and A. L. Stewart, Phil. Trans. Roy. Soc. London A **246**, 215 (1953).
[24] M. K. Chakrabarti, S. S. Bhattacharya, and S. Saha, J. Phys. B **21**, 3717 (1988).
[25] T. F. George, I. H. Zimmerman, J. M. Yuan, J. R. Laing, and P. L. DeVries, Acc. Chem. Res. **10**, 449 (1977); S. I. Chu, Chem. Phys. Lett. **54**, 367 (1978); A. D. Bandrauk and M. L. Sink, J. Chem. Phys. **74**, 1110 (1981); A. M. F. Lau, Phys. Rev. A **14**, 279 (1976).